

## RA・リサーチフェロー（博士研究員）・招聘外国人研究員・非常勤講師

本事業においては、博士研究員を下記要領で募集している。

### 募集案内

#### ポスドク募集



本研究教育拠点では、構成4部局の教官と協力して研究を行える方を募集しています。

研究内容の詳細は下記各部局のHPを参照してください。

- 理学研究科化学専攻 <http://kuchem.kyoto-u.ac.jp>
- 工学研究科分子工学専攻 <http://www.moleng.kyoto-u.ac.jp>
- 工学研究科合成・生物化学専攻 <http://sbchem.kyoto-u.ac.jp>
- 化学研究所 [http://www.kuicr.kyoto-u.ac.jp/index\\_J.html](http://www.kuicr.kyoto-u.ac.jp/index_J.html)

必ず、希望研究室の教官と直接コンタクトを取り、良くご相談の上でご応募ください。

#### 募集人員

若干名

#### 応募資格

博士号取得者または、採用時まで取得見込みの方

#### 応募期間

随時受付中

#### 提出書類

履歴書、業績リスト、これまでの研究概要（A4用紙1枚程度）、希望部局・研究室名、照会可能な方1名の氏名。以上を2部。

#### 書類提出先

600-8502 京都市左京区北白川追分町  
 京都大学大学院理学研究科化学専攻 齊藤軍治  
 「21世紀COE博士研究員応募」と朱書きのこと  
 電話 (075) 753-4035

#### 選考方法

書類審査及び面接により決定

これと並行して、研究・教育事業推進のためにRAを雇用し、また、外国人研究者を招聘した。平成14～16年度の実績と平成17年度の途中経過を下表にまとめた。

	RA	リサーチフェロー (括弧内は日本人)	招聘外国人研究員
平成14年度	26	7 (4)	12
平成15年度	81	17 (12)	4
平成16年度	99	21 (15)	8
平成17年度 (11月30日現在)	105	19 (13)	6

## Fu-Xue Chen (Department of Chemistry, Graduate School of Science)

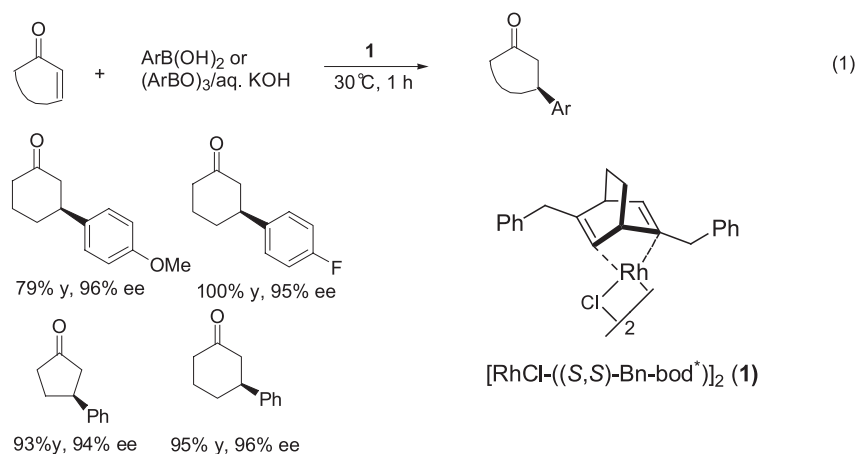


### Period

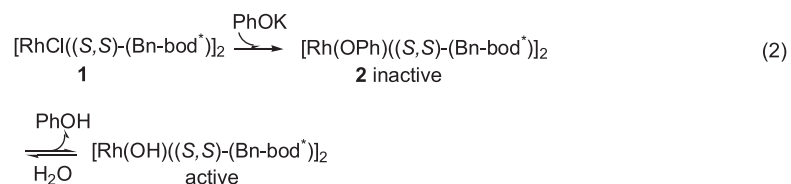
1 April, 2005~31 March, 2006

### Research

The recent development of chiral diene ligands opened a new research area in transition metal-catalyzed asymmetric reaction. They have been demonstrated to be highly effective ligands especially in rhodium-catalyzed aryl transfer reactions, but lower catalyst loading is still challenge as in other C-C bond forming transformations and has been rarely explored in literature. A new chiral diene-rhodium complex **1** was prepared and evaluated in the asymmetric 1,4-addition of arylboron reagents to  $\alpha, \beta$ -unsaturated ketones (eq. 1). Under the optimized conditions, with 0.005-0.01 mol% of **1**,  $\beta$ -substituted ketones were obtained in no less than 94% ee and up to 100% chemical yield. The optimum turnover frequency (TOF) was calculated to be  $1.4 \times 10^4 \text{ h}^{-1}$ , which is the highest one in catalytic asymmetric C-C bond-forming reactions. Moreover, this protocol can be performed at 18 mmol large scale without any loss in enantioselectivity, and thus exhibits potential industrial application.



It was found that phenol, which exists in commercially available phenyl boronic acid,  $\text{PhB}(\text{OH})_2$ , can deactivate the catalyst resulting in decrease of yield and even no product. Use of arylboroxine,  $(\text{ArBO})_3$ , can overcome this possible catalyst poisoning. The inactive complex **2** (eq. 2) in turn gave 1,4-adduct in only 11% yield but 96% ee. This observation provides profile information of the mechanism.



### Publications

1. "High Performance of a Chiral Diene-Rhodium Catalyst for the Asymmetric 1,4-Addition of Arylboroxines to  $\alpha, \beta$ -Unsaturated Ketones", F.-X. Chen, A. Kina, T. Hayashi, *Org. Lett.*, **8**, 341-344 (2006).



### Period

19 May, 2004 – 31 March, 2005

### Research

Coumarin (2*H*-1-benzopyran-2-one) and coumarin derivatives are naturally and synthetically important compounds. Asymmetric conjugate addition to coumarins is rarely explored. In our work, rhodium-catalyzed asymmetric addition of arylboronic acids to coumarins (Fig. 1) was investigated intensively. Three chiral diphosphine ligands (*R*)-Binap, (*R*)-P-Phos, and (*R*)-Segphos were tested in this reaction. (*R*)-Segphos was proved to be the best in enantioselectivity, while (*R*)-P-Phos performed better in activity. Influence of solvent, temperature and additives was investigated to optimize the reaction conditions. Several coumarin derivatives and a variety of arylboronic acids were synthesized and examined in this reaction. In most cases, good to excellent chemical yield and excellent enantioselectivity (up to 99% ee) were achieved under proper conditions. For example, in the presence of (*R*)-Segphos and Rh(acac)(C<sub>2</sub>H<sub>4</sub>)<sub>2</sub> (3 mol %), the reaction of 6-methylcoumarin **1** with phenylboronic acid at 60°C for 12 h gave 90% yield of (*R*)-3,4-dihydro-6-methyl-4-phenyl-2*H*-benzopyran-2-one **2** with 99.6% ee, which is a key intermediate in the synthesis of an important urological drug, (+)-(*R*)-Tolterodine **4** (Fig. 1).

Urinary incontinence is a condition affecting more than 10% of the adult population. (+)-(*R*)-Tolterodine **4** as a potent muscarinic receptor antagonist was hence marketed worldwide for treatment of urinary urge. Based on our results on rhodium-catalyzed asymmetric addition of arylboronic acids to coumarins, (+)-(*R*)-Tolterodine **4** can be synthesized asymmetrically.

Thus, treatment of **2** with diisobutylaluminumhydride (DIBAL) in toluene at -20°C afforded 90% yield of (*R*)-3,4-dihydro-6-methyl-4-phenyl-2*H*-benzopyran-2-ol **3**, which was consequently hydrogenated in the presence of 10% Pd-C in a mixture of methanol and diisopropylamine at 50 psi and 50°C to give 80% yield of (+)-(*R*)-Tolterodine **4**.

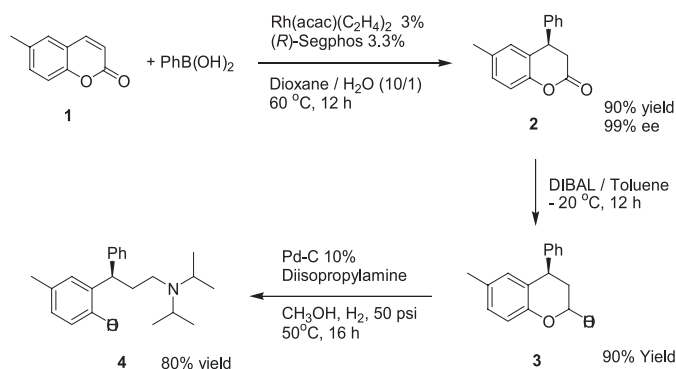


Figure 1 Rhodium-catalyzed asymmetric addition of arylboronic acids to coumarins and synthesis of (+)-(*R*)-Tolterodine

### Publications

“Rhodium-Catalyzed Asymmetric 1,4-Addition of Arylboronic Acids to Coumarins: Asymmetric Synthesis of (*R*)-Tolterodine”, G. Chen, N. Tokunaga, T. Hayashi, *Org. Lett.*, **7**, 2285-2288 (2005).

### 採用期間

平成17年6月1日～平成18年3月31日



### 研究報告

当研究室で開発されたキラル相間移動触媒 **1** (Figure 1) を用いるグリシン誘導体 **2** の  $\alpha$  位アルキル化反応は光学活性  $\alpha$ -アルキル  $\alpha$ -アミノ酸誘導体を高収率かつ高エナンチオ選択的に与え、生成物の加水分解により天然、非天然のアミノ酸を得ることが出来る (Scheme 1)。しかしながら工業的には、生成物をアミノ酸へと加水分解する際に生じるベンゾフェノン **2** の原料として再利用出来ないためコスト面で課題を残していた。一方でパラクロロベンズアルデヒドのシッフ塩基であるアラニン誘導体 **3** (Scheme 2) やグリシン誘導体 **4** (Table 1) は、加水分解で生成するパラクロロベンズアルデヒドを **3** や **4** の調製へと再利用出来る利点がある。

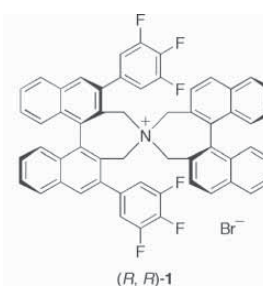
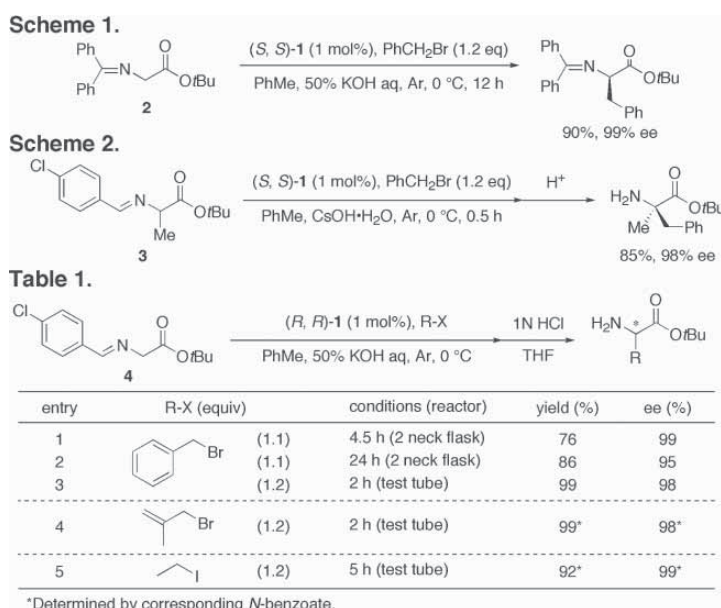


Figure 1

しかしながら工業的には、生成物をアミノ酸へと加水分解する際に生じるベンゾフェノン **2** の原料として再利用出来ないためコスト面で課題を残していた。一方でパラクロロベンズアルデヒドのシッフ塩基であるアラニン誘導体 **3** (Scheme 2) やグリシン誘導体 **4** (Table 1) は、加水分解で生成するパラクロロベンズアルデヒドを **3** や **4** の調製へと再利用出来る利点がある。しかしながら **3** が相間移動条件下でアルキル化されることから (Scheme 2)、**4** を  $\alpha$  位アルキル化反応の原料として用いた場合に、反応条件下において生成物のラセミ化や  $\alpha$  位ジアルキル化反応等の副反応が考えられる。そのため  $\alpha$  位アルキル化反応に **4** は適さないとされて来た。今回、光学活性  $\alpha$ -アミノ酸の実用的合成の実現へ向け、**4** を用いた相間移動条件下での不斉  $\alpha$  位アルキル化反応を研究課題とした。



まず初めにグリシン誘導体 **4** の不斉ベンジル化で検討を行った (Table 1)。相間移動触媒 (R, R)-**1** を 1mol% 用い、トルエン-50% KOH 水溶液中、アルゴン雰囲気下、**4** とベンジルブロミドを 0°C で 4.5 時間作用させた後、1N HCl 水溶液-THF で酸処理を行った結果、76% 収率、99% ee で生成物を得た (entry 1)。収率の向上を目指し、反応時間を 24 時間まで伸ばしてみたところ、収率は 86% まで改善されたものの予想された相間移動条件下での生成物のラセミ化が進行し選択性は 95% ee まで低下した (entry 2)。そこで、反応装置を替え攪拌効率を上げたところ、2 時間で反応は完結し 99% 収率、98% ee で目的とするフェニルアラニン誘導体を得た (entry 3)。最適化された反応条件を種々のアルキルハライドとの不斉  $\alpha$  位アルキル化反応に用いた結果、ベンジル化だけでなくアリル化やエチル化にも成功した (entries 4 and 5)。

## Chusaku Ikeda (Department of Chemistry, Graduate School of Science)



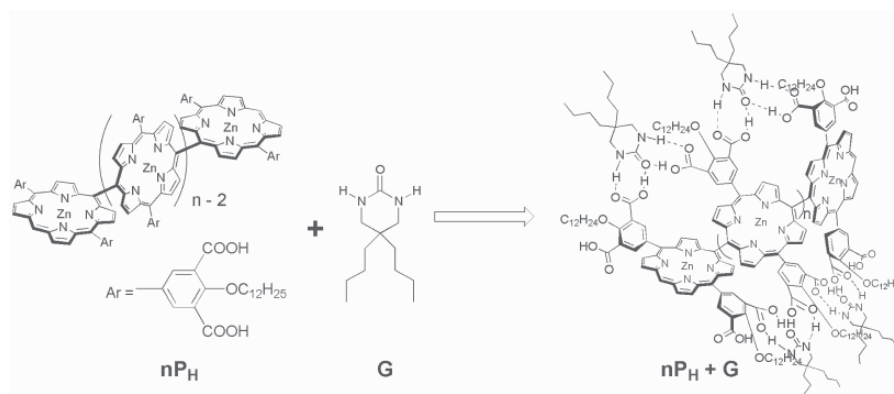
### Period

1 April, 2002 – 31 August, 2005

### Research

Well-defined porphyrin array that exhibit structural and/or conformational change as an response to a particular signal is quite attractive in view of their potential applicability as optical sensors due to the rich optical properties of porphyrin and the variety of strategy accessible to construct such systems. Among the enormous examples of multi-porphyrin systems, *meso, meso*-coupled porphyrin oligomers are particularly interesting because close proximity of the each porphyrin unit provides large electronic interactions that can be tuned by changing dihedral angle between porphyrin units.

In this study, we have investigated the *meso, meso*-coupled porphyrin oligomers that can be “helically-twisted” along the *meso, meso*-linkage by hydrogen bonding with guest molecules. Interestingly, resulted helical superstructure showed chiral amplification properties based on their helical conformation. *Meso, meso*-coupled porphyrin oligomers  $n\mathbf{P}_H$  ( $n = 2, 3, 4, 8$ ) bearing carboxyl moieties showed large spectral changes upon adding guest molecule  $\mathbf{G}$ . Detailed titration study including ester-derivative  $n\mathbf{P}_{Me}$  indicated that the observed spectral changes were caused by the decrease of dihedral angle between porphyrin plane from ca.  $90^\circ$  to a decreased angle by forming complementarily hydrogen bonding between carboxyl group of  $n\mathbf{P}_H$  and guest  $\mathbf{G}$ , resulting a helically twisted structure. The observed positive cooperativity in the guest binding event that was emphasized in the longer array also supported the helical structure. With the obtained helical superstructure in hand, we have found the handedness can be easily controlled by adding chiral amine that coordinate to zinc (II) center. Furthermore, intensities of the induced CD signal caused by adding chiral amine were much larger in  $n\mathbf{P}_H + \mathbf{G}$  system compared to  $n\mathbf{P}_H$  along or  $n\mathbf{P}_{Me}$ , which agreed well with the chiral enhancement mechanism through the helical backbone.



### Publications

“Helicity induction and two-photon absorbance enhancement in zinc (II) *meso, meso*-linked porphyrin oligomers via intermolecular hydrogen bonding interaction”, C. Ikeda, Z. S. Yoon, M.S Park, H. Inoue, D. Kim, and A. Osuka, *J. Am. Chem. Soc.*, **2005**, *127*, 534-535.

## Hiroto Kuninaka (Department of Chemistry, Graduate School of Science)

### Period

1 April, 2005 – 31 Mar, 2006



### Research

**(1) Contact problems and low-speed impacts of elastic materials.** The origin of irreversibility from a reversible mechanical model is one of the most fundamental subjects in non-equilibrium statistical mechanics. Although most of models discuss the transport processes under the influence of thermostats, we still do not understand the mechanism to reach an equilibrium state based on a purely mechanical model. Our aim is to derive macroscopic laws of elastic materials based on a microscopic lattice model. Our mechanical model is a two-dimensional spring-mass model with defect particles (Fig. 1). Using the model, we have carried out simulations of contact problems and quasistatic impact to show that our model can reproduce the Hertzian contact theory at equilibrium and the quasistatic theory for low speed impacts.

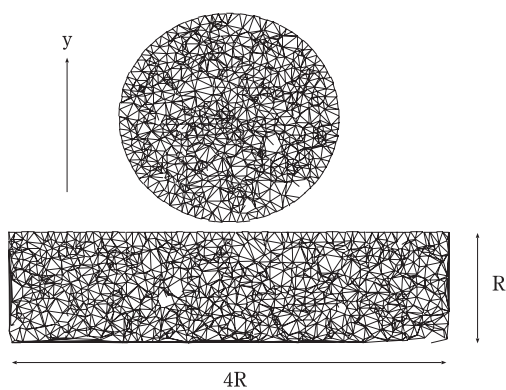


Fig. 1

**(2) Fracture dynamics of crystals.** The coherent phonon spectroscopy is used to investigate the atomic disarrangement in solids such as semiconductors, molecular crystals, etc. Our aim is to develop the method of the two-dimensional coherent phonon spectroscopy to investigate the fracture process of crystalline solids both theoretically and numerically. Now we are developing the MD simulator for the graphite consisted of 2304 carbon atoms (Fig. 2). By use of the simulator, we will investigate the relation between the signal of the coherent phonon spectroscopy and the internal state of the graphite under the external forces such as shears and compressions. In addition, we will extend the one-dimensional coherent phonon spectroscopy to the two-dimensional one to investigate the distribution of cracks generated from external forces.

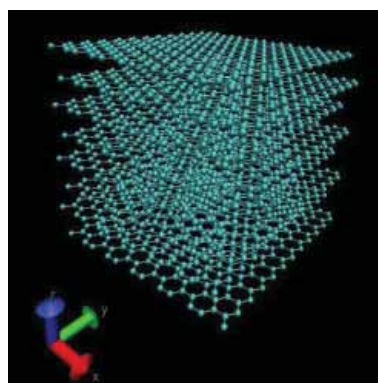


Fig. 2

### Publications

1. "Contact and Quasistatic impact of a Dissipationless Mechanical Model" **H. Kuninaka** and Hisao Hayakawa, *Powders & Grains 2005*. 2005, **2**, 1233-1236 (Rotterdam:Balkema, eds. by R. García-Rojo, H. J. Herrmann, and S. McNamara, ISBN : 041538348X).
  2. "Contact and Quasistatic impact of a Dissipationless Mechanical Model" **H. Kuninaka** and Hisao Hayakawa, to be submitted.
- Others : 1 article in preparation (to be appeared in "Bussei Kenkyu").

**Quanzhong Liu**  
(Division of Chemistry, Graduate School of Science, Kyoto University)



**Period**

1 April, 2005 ~ 31 May, 2005

**Research**

**Design of Environmentally Benign Chiral Phase-Transfer Catalysts.** Phase-transfer catalysis is a very useful approach that typically involves simple experimental operations, mild reaction conditions, inexpensive and environmentally benign reagents and solvents, and the large-scale reactions. Since the pioneering work of O'Donnell *et al.* in 1989, asymmetric synthesis of  $\alpha$ -amino acids by enantioselective alkylation of a prochiral protected glycine derivative using a chiral phase transfer catalyst has provided an attractive method for the preparation of both natural and unnatural amino acids. Recently, the Corey and Lygo groups independently reported an impressive departure from the previous results in terms of enantioselectivity and general applicability. However, almost all the elaborated chiral phase transfer catalysts reported so far have been restricted to cinchona alkaloid derivatives, which unfortunately constitutes a major difficulty in rationally designing and fine-tuning of catalysts to attain sufficient reactivity and selectivity for various chemical transformations under phase transfer catalyzed conditions. Accordingly, structurally rigid, chiral spiro-type (*R,R*)- or (*S,S*)-3,4,5-trifluorophenyl-NAS bromide derived from commercially available (*S*)- or (*R*)-binaphthol have been designed as a new  $C_2$ -symmetric chiral phase transfer catalyst and successfully applied to the highly efficient, catalytic enantioselective synthesis of both natural and unnatural  $\alpha$ -alkyl- and  $\alpha, \alpha$ -dialkyl- $\alpha$ -amino acids in enantiomerically pure form under mild phase transfer conditions.

**Publications**

1. Masanori Kitamura, Quanzhong Liu, Seiji Shirakawa, Yuichiro Arimura, and Keiji Maruoka, Combinatorial Design of New, Simplified Chiral Phase Transfer Catalysts for Practical Asymmetric Synthesis of  $\alpha$ -Alkyl- and  $\alpha, \alpha$ -Dialkyl- $\alpha$ -amino Acids, in preparation.



### 採用期間

平成 16 年 4 月 1 日～平成 17 年 3 月 31 日

### 研究報告

近年の超高速光パルスの発生技術の進歩により、複数の量子状態をコヒーレントに励起することによって量子核波束を形成し、その時間発展を観測することで高速反応の分光学的研究や光反応の制御の試みなどの研究が行われるようになった。本研究では、この核波束ダイナミクスの観測を理想的な孤立系である超音速ジェット中の分子クラスターに適用し、分子間ポテンシャルについての正確な情報を得ることを目的としている。本研究では、この核波束運動の観測法として位相がランダムな光パルス対を用いて、信号の揺らぎ(分散)から間接的に波束運動を観測する COIN 法および、one-color ポンプ-プローブ蛍光ディップ法を適用し核波束運動の観測を試みた。二つの方法を同時に適用することで励起状態だけでなく基底状態についての情報も同時に得られると期待される。

現在のところ、気相クラスターに対する実験の予備的段階として、超音速ジェット中の孤立分子に対する測定を行っている。その中の一例として、2-フルオロトルエンの蛍光ディップ及び COIN スペクトル(図 1 (a) 及び (b)) と、そのフーリエ変換を示した。スペクトルに現れたビートは、メチル基の内部回転運動波束の周期運動を反映したものである。各スペクトルのフーリエ変換には、確かに報告されている内部回転準位のエネルギー差と一致する周波数成分が現れることを確認した。また、蛍光ディップスペクトルは励起状態のエネルギー準位構造だけを反映した信号が現れるが、COIN スペクトルには励起状態と基底状態の情報が同時に現れるため、両スペクトルの振動数成分を比較することで両状態の準位構造が同時に得られることが実証できた。

現在、蛍光ディップ法を用いて基底状態の情報を得られるようにするために実験を進めている。

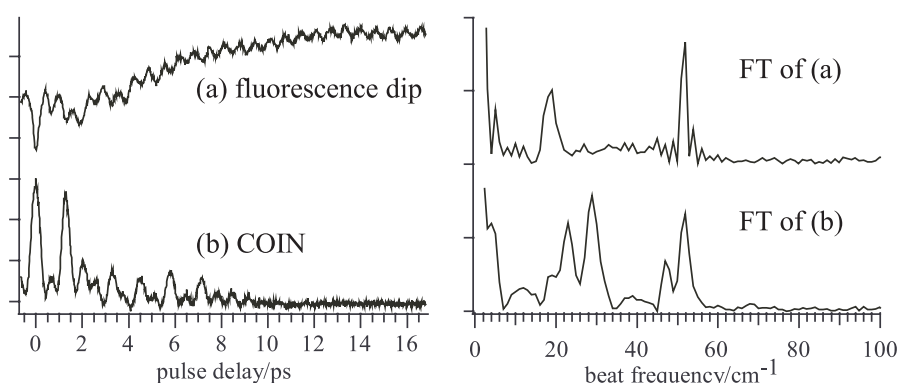


図 1 2-fluorotoluene の (a) 蛍光ディップ及び (b) COIN スペクトルとそのフーリエ変換

## Kenji Okamoto (Department of Chemistry, Graduate School of Science)



### Period

1 April, 2005 – 31 March, 2006

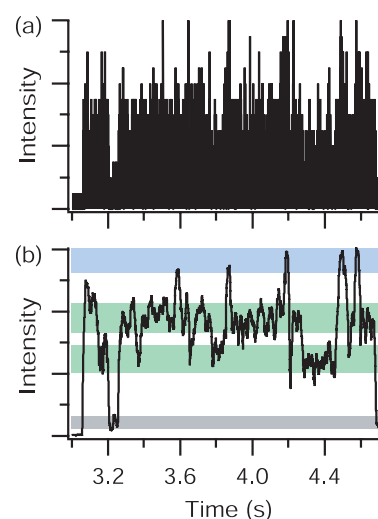
### Research

**(1) Measurement of dynamics of heme protein cytochrome *c*.** Cytochrome *c* (cyt *c*) protein has a heme-group, which includes a coordinate-bonded iron atom. Since it has the functionality of the charge transfer by oxidation and reduction of the iron atom, cyt *c* acts important roles at various situations in living body. It is also contained in thylakoid membrane and has an important role in the light harvesting system. Because of importance of its understanding, the dynamics of cyt *c* protein was investigated using single molecule measurement technique.

**(2) Observation of cyt *c* structure change via fluorescence.** A tetramethylrhodamine dye molecule is attached on a cyt *c* molecule. Due to the fluorescence resonance energy transfer (FRET) phenomenon, fluorescence intensity depends on dye-heme distance. Cyt *c* in compact native or molten-globule states shows almost no fluorescence. Denatured cyt *c* can be brighter. FRET allows us to detect the structure of the molecule through fluorescence signal. Confocal fluorescence microscope-based system was used for measurement. A photon counting module is employed as detector, which enables highly sensitive single molecule detection.

**(3) Measurement and results.** Cyt *c* molecules are prepared in glycine buffer (pH~2.5) with 0.2M NaCl. Because it is the middle of the denaturing condition (0M NaCl) and the molten-globule condition (0.4M NaCl), cyt *c* molecules are in equilibrium between those two states. Structure change arising from the state transitions was observed. Fluorescence image is first acquired to map locations of single cyt *c* adsorbed on the surface of glass substrate. Next, a time series of fluorescence signal from one of molecules is acquired.

Obtained signals usually contain unignorable shot noise, which is the statistical noise arising from randomness of fluorescence emission. An averaging scheme was developed in order to reduce the influence of this noise. The scheme defines the constraint on deviation of the signal, dynamically changes integration period and successfully extracts meaningful information from noisy signal. An example is shown in the figure, in which (a) an original jaggy signal was analyzed to extract (b) a smoothed curve. From the series of observations, it is found that there are intermediate state levels (indicated with green bands) between the dark molten-globule state level (indicated with a gray band) and the bright denatured state level (indicated with a blue band). This intermediate state is not observed in every transition. In some cases, direct transition between denatured and molten-globule states or cyt *c* molecules stay at intermediate states too shortly to be detected. Anyway, transitions are, in most cases, instantaneous jump to another state rather than gradual change.





**Period**

23nd November, 2004 – 29th November, 2005.

**Research**

The AppA protein in the purple bacterium *Rhodobacter Sphaeroides* interacts with photosynthesis repressor PpsR to form a stable AppA-(PpsR)<sub>2</sub> complex in the dark and in low light condition [1]. Blue light activated AppA can not associate with PpsR and therefore enable PpsR to bind to various promoters of the photosynthetic genes and inhibit the transcription [1]. Although AppA-mediated signal transduction is well understood, its initial photochemistry and structural transition leading to signaling state formation still remain to be solved. Time resolved transient grating (TG) is well established important technique to detect kinetics and conformational change which may occur near and/or away from the chromophore [2-4]. We have observed a faster dynamics (~2.3μs) in the TG spectra and this dynamics is independent of grating wavenumber (q<sup>2</sup>). This kinetics represents the relaxation from the excited triplet state. In the slower time scale of TG spectra, we have observed slow rise-decay component in low, middle and high q condition. The rate constant of both the rising and decay component depends on q<sup>2</sup>. Moreover, we have observed concentration dependency of TG signal in all q<sup>2</sup> condition. In going from low q<sup>2</sup> to high q<sup>2</sup> condition, the signal approaches to single exponential feature at very diluted condition. This concentration dependency feature indicates the aggregation

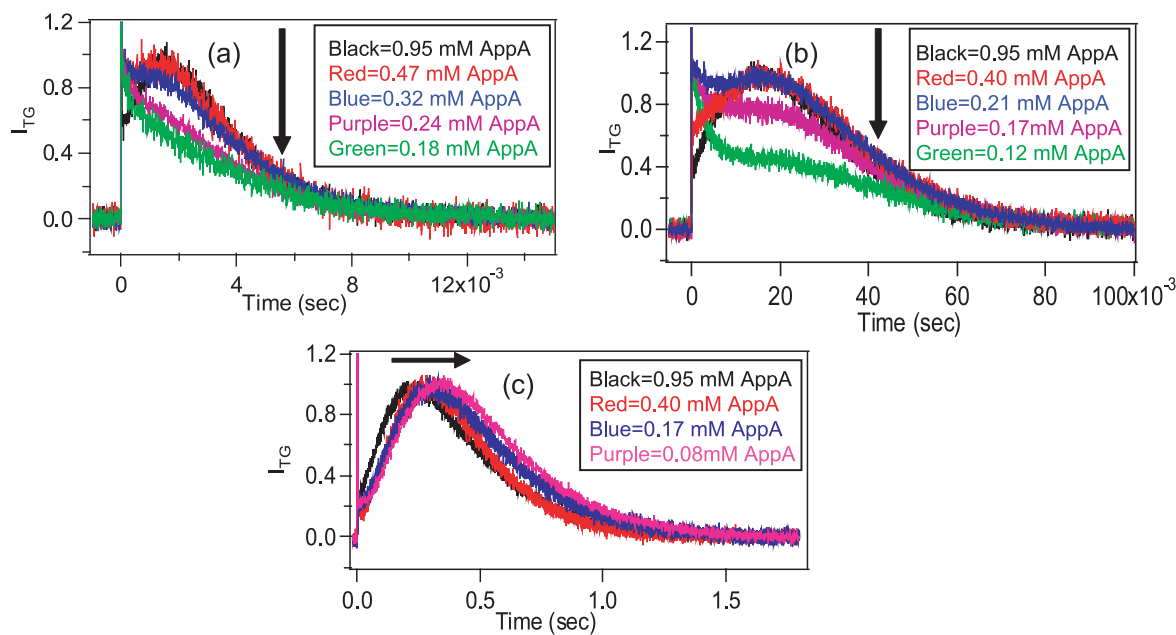


Fig. 1 TG signals of AppA in different concentration at (a)  $q^2 = 4.5 \times 10^{12} \text{ m}^{-2}$ , (b)  $q^2 = 5.6 \times 10^{11} \text{ m}^{-2}$  and (c)  $q^2 = 3.9 \times 10^{10} \text{ m}^{-2}$ .

process is occurring in the excited state of this protein. The possible interpretation of the observed TG signal is as follows. In the solution, parent AppA exists in monomer. By photo-irradiation, this protein changes its conformation, and dimer (or aggregation) is formed. At a higher concentration, this change occurs so quickly that we observe bi-exponential feature from the beginning at all  $q^2$  condition. But in the very diluted sample, the dimerization process becomes slower, as the parent molecules are far apart from each other. In the very fast time-scale (high  $q^2$  condition), this slow dimerisation kinetics can not be able to detect and as a result, reactant and product diffuses in the same rate and consequently we observed a single exponential feature. But in order to confirm above mentioned process, we have to analyse the TG signals in whole concentration range and in all  $q^2$  condition with a proper theoretical model. Hope, in near future we will able to analyse the TG signals with a suitable theoretical model and then it may give new insight to the photochemistry of this protein.

### References

- [1] M. A. Van Der Horst, K. J. Hellingwerf, *Acc. Chem. Res.* **2004**, 37, 13.
- [2] K. Takeshita, N. Hirota, Y. Imamoto, M. Kataoka, F. Tokunaga, M. Terazima, *J. Am. Chem. Soc.*, **2000**, 122, 8524.
- [3] M. Sakakura, S. Yamaguchi, N. Hirota, M. Terazima, *J. Am. Chem. Soc.*, **2001**, 123, 4286.
- [4] K. Inoue, J. Sasaki, M. Morisaki, F. Tokunaga, M. Terazima, *Biophys. J.*, **2004**, 87, 2587.

**R. V. S. S. N. Ravikumar**  
(Division of Chemistry, Graduate School of Science)



**Period**

December 3, 2003 – March 31, 2005

**A)** Optical and EPR spectral studies of transition metal bearing minerals and transition metal(TM) doped glasses have been carried out. Natural mineral sodalite, microcline, perthite and several TM-doped phosphate and borate glasses characterized by EPR (CW-ESR, X-Band, Q-band, Pulsed ESR) were investigated at various temperatures (from room temperature to 4K), and their optical absorptions studied. Several interesting results have been presented at the national and international conferences, and research papers were communicated in journals listed below.

- 1) Octahedral and tetrahedral sites of different iron bearing natural minerals spectral studies: **R.V.S.S.N.Ravikumar** & Jun Yamauchi presented as **oral** talk at 8<sup>th</sup> ESR Niigata University, Niigata (Japan) June 11-12, 2004.
  - 2) EPR of Cr<sup>3+</sup> doped zinc phosphate glass : **R.V.S.S.N.Ravikumar**, J.Yamauchi,A.V.Chandrasekhar, P.S.Rao & Y.P.Reddy presented as **poster** at APES international school held at Mumbai (India) during Nov. 17 to 20, 2004.
  - 3) Tetrahedral site of Fe(III) ions in natural sodalite from Brazil: A.V.Chandrasekhar, Y.P.Reddy, B.J.Reddy, P.S.Rao, **R.V.S.S.N.Ravikumar** & J.Yamauchi.
  - 4) Bonding nature of Cr<sup>3+</sup> and Ni<sup>2+</sup> doped zinc phosphate glasses: Y.P.Reddy, **R.V.S.S.N.Ravi kumar**, A.V.Chandrasekhar, P.S.Rao & J.Yamauchi.
  - 5) EPR and optical studies on VO<sup>2+</sup> doped ARbB<sub>4</sub>O<sub>7</sub> (A=Li, Na, K) glasses : **R.V.S.S.N. Ravikumar**, A.V.Chandrasekhar, Y.P.Reddy, R.Komatsu, K.Ikeda, P.S.Rao & J.Yamauchi.
  - 6) Spectral studies of natural incrustation material grown in wells : Rayalaseema region of Andhara Pradesh, India:Y.Srinivasa Rao, A.V.Chandrasekhar, Y.P.Reddy, P.S.Rao, **R.V.S.S.N.Ravikumar** & J.Yamauchi.
- Above (3-6 Papers) Presented as Oral talks at 4<sup>th</sup> Asia-Pacific EPR/ESR symposium (APES'04), Indian Institute of Sciences (IISc.) Bangalore (India), Nov. 22-25 (2004).
- 7) Identification of chromium and nickel sites in zinc phosphate glasses : **R.V.S.S.N.Ravikumar**, J.Yamauchi, A.V.Chandrasekhar,Y.P.Reddy & P.S.Rao: Journal of Molecular Structure (UK), 740, 169-173(2005).
  - 8) Tetrahedral site of iron in natural mineral sodalite, **R.V.S.S.N.Ravikumar**, A.V.Chandrasekhar, J.Yamauchi, Y.P.Reddy & P.S.Rao: Radiation Effects & Deffects in Solids, in print (2005).

**B)** In addition to **A)** intense researches was carried out till the end of my period of stay on nano forms of semiconductors materials such as nanoparticles, nanowires and nanotubes to find suitable components for future miniature electronic devices. Much effort has been made to the syntheses of nanomaterials with different shapes, such as nanowires, nanobelts, nanocubes and nanotubes. Nanowires and nanotubes could be important for the constituents of such devices as interconnects, or the devices could be integrated on nanowires and nanotubes. In corporation of guest atoms in such quasi one dimensional system during the growth process could make it possible to produce nanowires and nanotubes with novel structures and wide ranging electric and magnetic properties. After finishing characterizations of these materials, including optical and ESR spectroscopies, these results are now being summarized for publication in several journals.

## Masafumi Sakata (Division of Chemistry, Graduate School of Science)

### Period

1 April, 2003 – 31 March, 2006



### Research

**(1) The effect of uniaxial strain on  $(\text{EDO-TTF})_2\text{PF}_6$ .** The quasi-one dimensional organic conductor  $(\text{EDO-TTF})_2\text{PF}_6$  shows the novel metal-insulator transition at ca. 280 K. I have examined the influence of the uniaxial strains on the novel metal-insulator transition of  $(\text{EDO-TTF})_2\text{PF}_6$  by means of the transport measurements. The small strain along the intralayer direction slightly suppressed the transition, while that along the interlayer direction assisted distinctly. The present results suggest that the electrostatic interaction between the positive charge on the donor molecule and the negative charge on the anion plays an important role in the transition. I have also found that the first-order transition was suppressed by the large strain along each direction. The phase around room temperature showed small temperature dependence of resistivity and the transition to insulating phase occurred with the feature of second-order transition.

**(2) Preparation of superconducting  $(\text{TMTSF})_2\text{NbF}_6$  using ionic liquid.** High quality single crystals of an organic superconductor  $(\text{TMTSF})_2\text{NbF}_6$  were prepared using a room temperature ionic liquid 1-ethyl-3-methylimidazolium  $\cdot \text{NbF}_6$  as electrolyte. The crystal is isostructural to the other members of TMTSF superconducting family  $(\text{TMTSF})_2\text{X}$  with octahedral anions X. The salt exhibited a metal-insulator transition at 12 K due to the spin density wave formation at ambient pressure and became superconducting with  $T_c = 1.26$  K (on-set) at  $P_c = 1.2$  GPa.

**(3) Physical properties of  $(\text{ET})_3(\text{AuBr}_2)_2(\text{AuBr}_4)_2$ .** The transport, and optical properties of the novel salt,  $(\text{ET})_3(\text{AuBr}_2)_2(\text{AuBr}_4)_2$ , having a peculiar structure of the conducting layer which consists of ET and AuBr<sub>2</sub> molecules, are investigated. This salt showed the metallic behavior down to ca. 100 K with the room temperature conductivity of  $10 \text{ Scm}^{-1}$ . The semiconducting behavior was observed below 100 K. The reflectance spectrum polarized parallel to the donor layer showed the Drude-like feature at room temperature and the small gap appeared below 100 K. These features are consistent with the result of transport measurement. Raman and infrared spectra polarized perpendicular to the donor layer suggest the charge disproportionation in spite of the metallic conductivity. The slight charge redistribution was observed below 100 K.

### Publications

1. "Uniaxial strain investigation on the metal-insulator transition of  $(\text{EDO-TTF})_2\text{PF}_6$ " M. Sakata, M. Maesato, A. Ota, H. Yamochi, G. Saito, *Synthetic Metals*, 2005, **153**, 393-396.
2. "Preparation of superconducting  $(\text{TMTSF})_2\text{NbF}_6$  by electrooxidation of TMTSF using ionic liquid as electrolyte" M. Sakata, Y. Yoshida, M. Maesato, G. Saito, K. Matsumoto, R. Hagiwara, *Mol. Cryst. Liq. Cryst.*, in press.

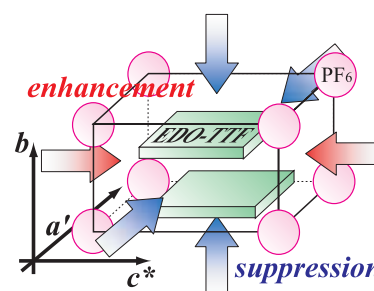


Fig. 1 Schematic representation of the applied directions of uniaxial strain.  $a'$ ,  $b$  axis are in the intralayer direction and  $c^*$  axis is parallel to the interlayer direction.

**Satoshi Shimono** (Department of Chemistry, Graduate School of Science, Kyoto University)

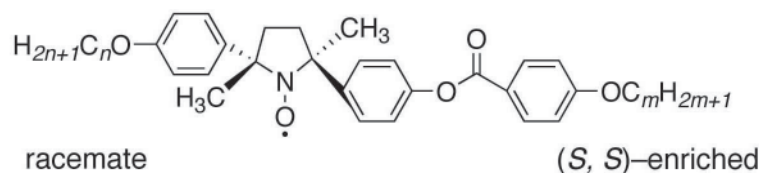


**Period**

1 April, 2005 – 31 March, 2006

**Research**

**Molecular Orientation of Chiral Organic Radical Liquid Crystals (LCs).** The molecular orientation of novel racemic and nonracemic cyclic nitroxides (*e.g.* **1** and **2**) showing smectic C (SmC) or chiral smectic C (SmC\*) liquid crystalline phases was investigated by means of X-band CW-EPR spectroscopy (ca. 0.33T).



<b>1:</b> $m = n = 13$ : C 68.7 <b>SmC</b> 84.8 N 88.6 I	<b>1:</b> $m = n = 13$ : C 64.0 <b>SmC*</b> 85.0 <b>N*</b> 89.8 I
<b>2:</b> $m = 8, n = 7$ : C 63.3 N 103.1 I	<b>2:</b> $m = 8, n = 7$ : C 79.3 <b>N*</b> 103.5 I

**Scheme 1.** Structures of LC molecules and their phase transition temperatures (°C).

During the heating process, the *g* value of (±)-**1** slightly increased on the crystal-to-SmC phase transition. From the anisotropy of the *g* value of the nitroxide radical, the observed increase in *g* value is ascribed to the change of molecular alignment; the N–O axis is close to parallel to the applied magnetic field. This behavior is in contrast to that of (±)-**2** in the nematic (N) phase, which shows the molecular alignment that the N–O axis is perpendicular to the direction of the magnetic field. As in the case of (±)-**1**, slight increase of *g* value was observed on the crystal-to-SmC\* phase transition of (*S, S*)-**1**. This indicates that the molecules align in such a way that the N–O axis is close to parallel to the applied magnetic field. Further details of the molecular orientation and properties of di- and trinitroxide derivatives of **1** are now under investigation.

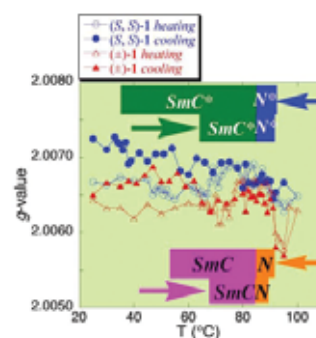


**Fig. 1** Temperature dependence of the *g* value for **1**; measured through the first heating and cooling processes.

**Publication**

"Ferroelectric Properties of Paramagnetic, All-Organic, Chiral Nitroxyl Radical Liquid Crystals" N. Ikuma, R. Tamura, **S. Shimono**, Y. Uchida, K. Masaki, J. Yamauchi, Y. Aoki, H. Nohira, *Adv. Mater.*, *in press*.

**Presentations**

- "Molecular Orientation of Chiral Organic Radical Liquid Crystals in the Bulk State" **S. Shimono**, J. Yamauchi, N. Ikuma, Y. Noda, R. Tamura, The 44th Annual Meeting of the Society of Electron Spin Science and Technology (SEST2005), Sendai, Japan, October 2005.
- "Molecular Orientation of Chiral Paramagnetic Organic Liquid Crystals in a Magnetic Field" **S. Shimono**, R. Tamura, N. Ikuma, J. Yamauchi, 4th International Conference on Nitroxide Radicals: Synthesis, Properties and Implications of Nitroxides (SPIN-2005), Novosibirsk, Russia, September 2005.

## Shin Takahashi (Surface Chemistry Laboratory, Division of Chemistry, Graduate School of Science)

### Period

1 April, 2004 – 31 March, 2006



### Research

Ru(0001) surface oxidation mechanism was studied by use of oxygen supersonic molecular beam (SSMB) and high resolution X-ray photoemission spectroscopy. An oxygen covered ruthenium surface attracts wide attentions from research area of surface science, material science and industrial chemistry as in fuel cell technology due to its catalytic activity of carbon monoxide oxidation. The present study mainly focused on the effect of vibrational excitation of oxygen molecules to oxidation process on oxygen precovered Ru(0001) surface with a coverage of half monolayer (ML) which corresponds to  $p(2 \times 1)$  structure. At this point, it is well known that oxygen adsorption probability rapidly decreases.

All experiments were performed at surface chemistry end-station, a soft X-ray beam line, BL23SU in SPring-8. Oxygen precovered Ru(0001) surface with a coverage of 0.5 ML was prepared by exposing oxygen less than several tens of Langmuir at room temperature and then brief heating to 573 K to achieve well ordered surface. High energy  $O_2$  SSMBs was generated by adiabatic expansion of mixture of  $O_2$  and carrier gases such as helium and argon. In order to examine a vibrational excitation effect, a nozzle temperature was set at 300 K (denoted as RT 0.5 eV) or 1400 K (denoted as HT 0.5 eV) with a translational energy keeping at 0.5 eV by changing a mixing ratio of carrier gases. Photoemission spectra of Ru  $3d_{5/2}$  and O  $1s$  were measured by monochromatic synchrotron radiation beam with photon energy of 340 eV and 650 eV, respectively. Detection angle of photoelectrons was 70 degree with respect to surface normal. In such condition, escape depth of photoelectron was limited in several angstrom from surface. Half monolayer of oxygen precovered surface with  $p(2 \times 1)$  phase was identified by the presence of S1(2O) and the absence of S1 and S1(3O) components in the Ru  $3d_{5/2}$  photoemission peak, where S1, S1(2O) and S1(3O) are first layer ruthenium atoms bound to no, two and three oxygen atoms, respectively. Relative oxygen coverage was estimated by O  $1s$  photoemission peak area based on that of half monolayer sample.

Fig. 1 shows oxygen uptake curves when irradiating RT 0.5 eV and HT 0.5 eV SSMBs onto 0.5 ML oxygen precovered Ru(0001) surface. Uptake curve for HT 0.5 eV showed higher adsorption probability in comparison with that for RT 0.5 eV, i.e., a vibrational excitation by heating a nozzle induces higher adsorption probability. In the present oxygen coverage region, Ru  $3d_{5/2}$  surface core level spectra gave intermediate structure between  $p(2 \times 1)$  phase and  $(2 \times 2)$ -3O phase with three oxygen atoms per unit cell. In every case, no particular oxidation state on ruthenium surface was induced by vibrationally excited oxygen or by high energy SSMBs.

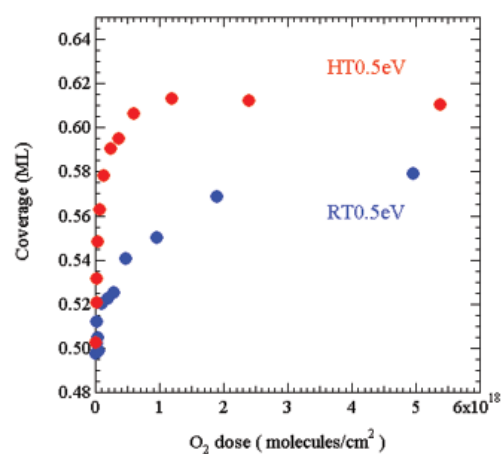


Fig. 1 Oxygen uptake curves for HT and RT 0.5 eV onto 0.5 ML oxygen precovered Ru(0001) surface.

## Zhang Wen (Lab of Chemical Biology, Division of Chemistry, Graduate School of Science, Kyoto University)

### Period

10 December, 2003 – 31 December, 2005



### Research

Pyrrole-imidazole (Py-Im) polyamides can better recognize a predetermined DNA sequence in the B-DNA minor groove, alkylate DNA at a specific site by an alkylating agent, and enter living cells toward possible chemical regulation of gene expression. To date, all the four Watson-Crick base pairs can be recognized using different pairings of three aromatic amino acids, with an Im/Py pairing reading G·C, a Py/Im pairing reading C·G, and an Hp/Py pairing being able to distinguish T·A from A·T, G·C and C·G, whereas with a Py/Py pairing nonspecifically discriminating both A·T and T·A from G·C and C·G, which are common recognition rules by polyamides in the DNA minor groove.

However, in some cases, relatively subtle structural changes in hairpin polyamide design may result in relatively large changes in DNA binding mode or sequence selectivity. The modification and the displacement of central monomer and N- and C-terminal functionalization of polyamides have shown to greatly affect their DNA binding affinity and sequence selectivity, but in our knowledge, little was reported on the impact of  $\alpha$ -substituted  $\gamma$ -turn of polyamides on the DNA minor groove recognition, i.e. specifically discriminating four Watson-Crick base pairs, T·A, A·T, C·G and G·C at turn position with  $\alpha$ -substituents in  $\gamma$ -turn.

The research examines and highlights the effect of stereochemistry of  $\alpha$ -substituents in  $\gamma$ -turn on the DNA base binding selectivity at turn position.

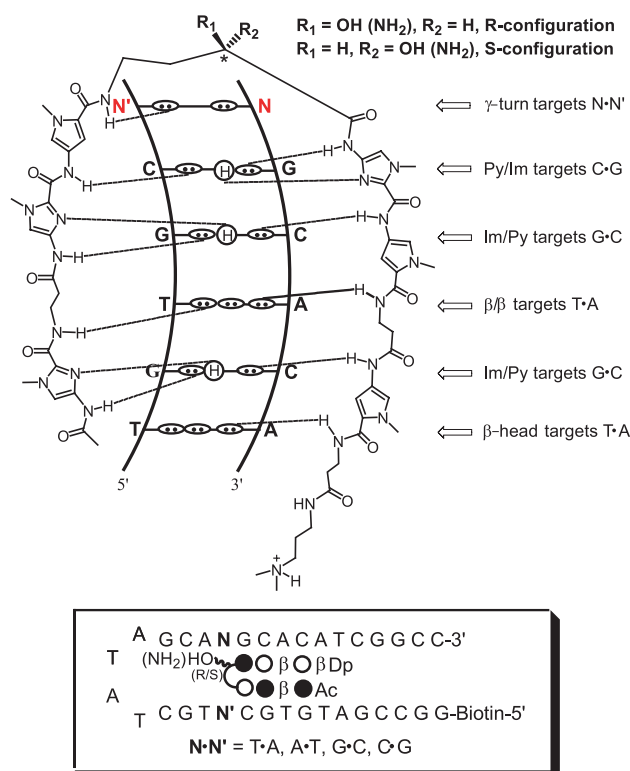


Fig. 1 Molecular recognition model of polyamides to sequence-specific DNAs in the minor groove. Ellipses with dots represent lone pairs of N3 of purines and O2 of pyrimidines. Hydrogen bonds are shown as dotted lines. Circles containing an H represent the N2 hydrogen of guanine. A ball model for the complexes is given in a box at the bottom. Imidazole residue (Im) is black circles, pyrrole residue (Py) is open circles,  $\beta$  represents  $\beta$ -alanine residue, Dp represents dimethylamino-propylamide,  $\gamma$  represents  $\gamma$ -aminobutanoic acid turn residue connecting the two subunits, and Ac is acetyl.

As shown in Figure 1, we designed four  $\alpha$ -substituted  $\gamma$ -aminobutyric acid residues: (R or S)- $\alpha$ ,  $\gamma$ -diaminobutyric acid ( $^R\gamma_{\alpha-NH_2}$  or  $^S\gamma_{\alpha-NH_2}$ ), (R or S)- $\alpha$ -hydroxyl- $\gamma$ -aminobutyric acid ( $^R\gamma_{\alpha-OH}$  or  $^S\gamma_{\alpha-OH}$ ), as base recognition elements at  $\gamma$ -turn position in the construction of polyamides, based on different stereochemical properties of  $\alpha$ -substituents in  $\gamma$ -turn. The binding properties of designed polyamides to selected hairpin DNA, including binding affinity, specificity, stoichiometry, kinetics and thermodynamics, were investigated with Biacore SPR technique (Table 1).

As can be seen in Table 1, S- $\gamma$ -turn linked hairpin polyamide **3** binds more weakly to four bases T·A, A·T, C·G, G·C than R- $\gamma$ -turn linked hairpin polyamide **2** with reduced affinities of 35-fold, 200-fold, 18-fold, and 283-fold, respectively. A combination of several factors may determine binding affinity of the polyamide **2** to four base pairs and 4.5-fold specificity for discrimination of T·A from A·T. More importantly, we find that (S)- $\alpha$ -hydroxyl-modified- $\gamma$ -turn linked hairpin polyamide **3** favorably binds to the sequence with T·A at turn position over that with A·T with a 25-fold specificity. Dervan et al showed  $\alpha$ -prechiral hydrogen in the  $\gamma$ -turn has a NOE contact with C1'H of 3'-end of the nucleotide adjacent to bases at the turn position by NMR method due to the proximity of the proton to the nucleotide. So, when hydroxyl substituent is S-configuration, it quite possibly induces formation of hydrogen bonding with N3 of 3'-G adjacent to bases at the turn position, as stated in the previous research. Also there is another possibility that (S)- $\alpha$ -hydroxyl is in favorable orientation to able to form a hydrogen bonding with O2 of T base at turn position. One of the above two factors may mainly determine the binding selectivity to T·A, A·T, C·G, and G·C.

In summary, the novel polyamides with  $\gamma$ -turn modification were designed and their recognition properties including affinity, selectivity, stoichiometry and kinetics properties to four DNA base pairs were evaluated in detail by BIACORE Technique. Results show that the (S)- $\alpha$ -hydroxyl- $\gamma$ -turn can discriminate T·A from A·T, C·G and G·C. Examination of recognition properties of the polyamides with (R/S)- $\alpha$ -amino- $\gamma$ -turn is proceeding.

Table 1 Dissociation equilibrium constants ( $K_D$ ) for binding

Polyamide	$K_D$ (nM)				Note <sup>a</sup>
	T·A	A·T	G·C	C·G	
 <b>1</b>	26(119 <sup>b</sup> )	22(140)	150(20)	3100	0.85
 <b>2</b>	3.1(277)	14(61)	120(7.2)	860	4.5
 <b>3</b>	110(145)	2800(5.7)	34000(0.47)	16000	25

<sup>a</sup> The value was defined as  $K_D(A·T)/K_D(T·A)$ , indicating the difference of binding affinity between T·A and A·T.

<sup>b</sup> Specificity:  $K_D(C·G)/K_D(N·N')$ ,  $N·N' = T·A, A·T, G·C$ .

## Publications

1. Hiroyuki Matsuda, Noboru Fukuda, Takahiro Ueno, Yoshiko Tahira, Hirohito Ayame, **Wen Zhang**, Toshikazu Bando, Hiroshi Sugiyama, Satoshi Saito, Koichi Matsumoto, Hideo Mugishima, and Kazuo Serie. *Development of gene silencing pyrrole-imidazole polyamide targeting the TGF-beta 1 promoter for treatment of progressive renal diseases*. J Am Soc Nephrol. **2005**. In press.
2. **Wen Zhang**, Toshikazu Bando and Hiroshi Sugiyama. *Discrimination of hairpin polyamides with an  $\alpha$ -substituted- $\gamma$ -aminobutyric acid as a TG-reader in DNA minor groove*. Submitted.

## Michinori Sumimoto (Department of Molecular Engineering, Graduate School of Engineering)



### Period

1 April, 2003 – 31 March, 2005

### Research

(1) Various interesting geometries have been reported in silyl-, silylene-, and silane-bridged dinuclear transition metal complexes. For instance, dinuclear Rh(II) complex takes silyl-bridged form 1 when chelate phosphine coordinates with Rh, while it takes symmetrical form 2 when monodentate phosphine coordinates with Rh. We theoretically investigated  $[\text{RhL}(\mu\text{-SiH}_2)(\text{H})_2]_2$  ( $\text{L} = \text{PH}_3, \text{PH}_2\text{CH}_2\text{CH}_2\text{PH}_2$ ) with the DFT method to clarify geometry, bonding nature, and electronic structure. In the monodentate phosphine complex, the silyl-bridged form and the silylene-bridged form exist as stable species. There is one transition state connecting these two structures. In the silyl-bridged form, the dihedral angle between the two Rh-Si-Rh planes is  $113^\circ$ . In the silylene-bridged form, two Rh atoms and two Si atoms are on the same planes and four Rh-Si bonds are almost equivalent. DFT/B3LYP and CCSD (T) calculation show that both the silyl-bridged form and silylene-bridged form are very close in energy and the interconversion between two structures easily occur with a small activation barrier. On the other hand, in the chelate phosphine dinuclear Rh complex, the silyl-bridged form exists as stable species. The silylene-bridged form in the chelate phosphine complex becomes a transition state. In the silylene-bridged form, the difference between the monodentate phosphine complex and the chelate phosphine complex can understand from molecular orbital. In the chelate phosphine complex, lone pair orbital of P atom and d orbital of Rh atom form the antibonding orbital. From these results, the silylene-bridged form in the chelate phosphine complex is not stable and becomes a transition state.

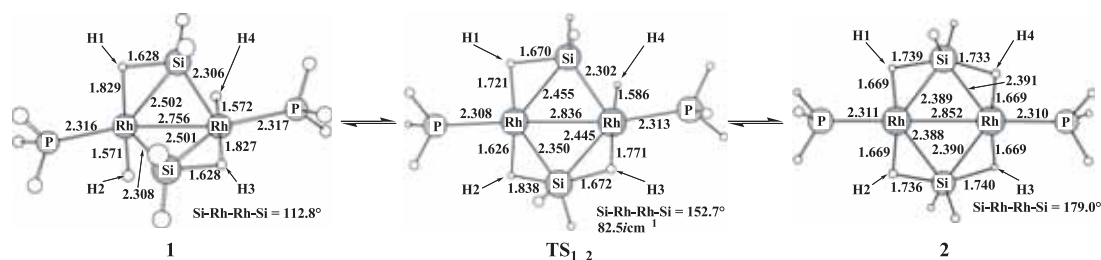


Fig. 1 DFT-optimized structures of  $[\text{Rh}(\text{PH}_3)(\mu\text{-SiH}_2)(\text{H})_2]_2$ .

### Publications

- “Electronic structures of unoccupied states in lithium phthalocyanine thin films of different polymorphs studied by IPES” K. Tsutsumi, H. Yoshida, N. Sato, **M. Sumimoto**, H. Fujimoto and S. Sakaki, *Appl. Surf. Sci.*, 2003, **212-213**, 438-440.
  - “Theoretical Study of the Cp2Zr-Catalyzed Hydrosilylation of Ethylene Reaction Mechanism Including New  $\sigma$ -Bond Activation” S. Sakaki, T. Takayama, **M. Sumimoto** and M. Sugimoto, *J. Am. Chem. Soc.*, 2004, **126**, 3332-3348.
  - “Theoretical Study of Trans-metalation Process in Palladium-Catalyzed Borylation of Iodobenzene with Diboron” **M. Sumimoto**, N. Iwane, T. Takahama and S. Sakaki., *J. Am. Chem. Soc.*, 2004, **126**, 10457-10471.
- Others : 1 articles in preparation.

隅本 倫徳 (すみもと みちのり)  
工学研究科分子工学専攻分子物性工学研究室



採用期間

平成 15 年 4 月 1 日～平成 17 年 3 月 31 日

研究報告

シリル、シリレンなどのケイ素化学種が架橋した多くの二核金属錯体の構造は多様性に富んでいる。例えば、ケイ素架橋二核ロジウム錯体の場合、ホスフィン部位のわずかな相違により構造が大きく異なる。これは錯体の多様性を示すものであり、ホスフィンの相違が構造と電子状態を変化させると考えられ、興味を持たれる。本研究では、ケイ素架橋二核ロジウム錯体  $[\text{RhL}(\mu\text{-SiH}_2)(\text{H})_2]_2$  ( $\text{L} = \text{PH}_3, \text{PH}_2\text{CH}_2\text{CH}_2\text{PH}_2$ ) の構造、結合性、電子状態を理論計算によって解明することを目的とした。単座ホスフィン二核ロジウム錯体の場合、二つの  $\text{Rh-Si-Rh}$  面のなす二面角が  $113^\circ$  と折れ曲がったシリル架橋構造と、 $\text{Rh}$  と  $\text{Si}$  がほぼ同一平面上に存在するシリレン架橋構造の二つの構造が安定に存在できることがわかった。また、二つの安定構造のエネルギー差は非常に小さく、周囲の状況に応じていずれの構造も取り得ることが示された。一方、キレートホスフィン二核ロジウム錯体の場合、折れ曲がったシリル架橋のみが安定構造となり、シリレン架橋構造は遷移状態として存在することがわかった。また、活性障壁は  $26.1 \text{ kcal/mol}$  と非常に高く、構造変換は困難である。シリレン架橋錯体の安定性の違いは、分子軌道から理解できる。キレートホスフィン錯体では、四つの  $\text{P}$  の lone pair と二つの  $\text{d}$  軌道から反結合性軌道が形成され、軌道の不安定化が起こる。一方、単座ホスフィン錯体では、 $\text{P}$  の lone pair の影響をほとんど受けない。このためキレートホスフィンシリレン架橋錯体は不安定化し、遷移状態となること明らかとなった。

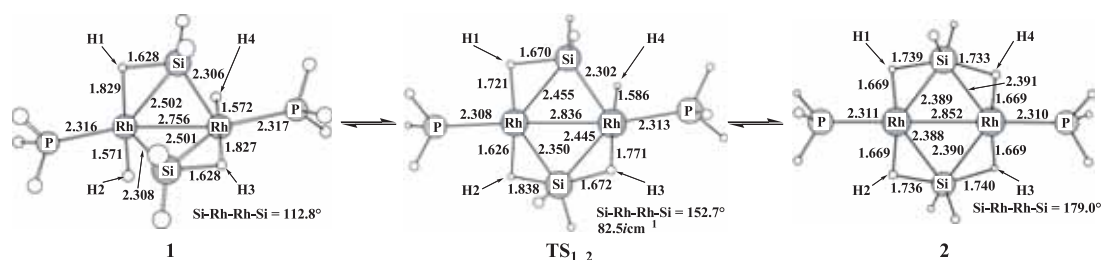


図 1 DFT/B3LYP 法で最適化した  $[\text{RhL}(\mu\text{-SiH}_2)(\text{H})_2]_2$  の構造変化

論文発表

- “Electronic structures of unoccupied states in lithium phthalocyanine thin films of different polymorphs studied by IPES” K. Tsutsumi, H. Yoshida, N. Sato, **M. Sumimoto**, H. Fujimoto and S. Sakaki, *Appl. Surf. Sci.*, 2003, **212-213**, 438-440.
- “Theoretical Study of the Cp2Zr-Catalyzed Hydrosilylation of Ethylene Reaction Mechanism Including New  $\sigma$ -Bond Activation” S. Sakaki, T. Takayama, **M. Sumimoto** and M. Sugimoto, *J. Am. Chem. Soc.*, 2004, **126**, 3332-3348.
- “Theoretical Study of Trans-metalation Process in Palladium-Catalyzed Borylation of Iodobenzene with Diboron” **M. Sumimoto**, N. Iwane, T. Takahama and S. Sakaki., *J. Am. Chem. Soc.*, 2004, **126**, 10457-10471.

その他：投稿準備中 1

# Ryoichi Fukuda (Department of Synthetic Chemistry and Biological Chemistry, Graduate School of Engineering)



## Period

1 April, 2005 – 31 March, 2006

## Research

### (1) Relativistic and electron correlation effects on the NMR chemical shift of heavy elements:

Magnetic properties The quasi-relativistic (QR) generalized unrestricted Hartree-Fock (GUHF) method for the magnetic shielding constant has been extended to include the electron correlation effect in the level of the second-order Møller-Plesset perturbation (MP2) theory. We have implemented the energy gradient and finite-perturbation methods to calculate the magnetic shielding constant at the QR MP2 level and applied to the magnetic shielding constants and the NMR chemical shifts of  $^{125}\text{Te}$  nucleus in various tellurium compounds. The calculated magnetic shielding constants and NMR chemical shifts well reproduced the experimental values. The relations of the chemical shifts with the natures of ligands,

and the tellurium oxidation states were investigated. The chemical shifts in different valence states were explained by the paramagnetic shielding and spin-orbit terms. The tellurium 5p-electrons are the dominant origin of the chemical shifts in the Te(I) and Te(II) compounds and the chemical shifts were explained by the p-hole mechanism. The tellurium d-electrons also play an important role in the chemical shifts of the hyper-valent compounds.

**(2) Direct algorithm for SAC/SAC-CI method:** The SAC/SAC-CI method is the electron correlation theory for the various electronic states and the SAC/SAC-CI method was presented to wide researchers on the Gaussian 03 program suit. In this study, we developed an efficient algorithm for the SAC/SAC-CI calculations. The direct algorithm has been adopted for the calculation of the SAC/SAC-CI analytical energy gradient method.

## Publications

- "Quasirelativistic theory for the magnetic shielding constant. III. Quasirelativistic second-order Møller-Plesset perturbation theory and its application to tellurium compounds", R. Fukuda, H. Nakatsuji, *J. Chem. Phys.* **123**, 044101-1-10 (2005)
- "Relativistic configuration interaction and coupled cluster methods using four-component spinors: Magnetic shielding constants of HX and CH<sub>3</sub>X (X = F, Cl, Br, I)" M. Kato, M. Hada, R. Fukuda, H. Nakatsuji *Chem. Phys. Lett.* **408**, 150-156 (2005)

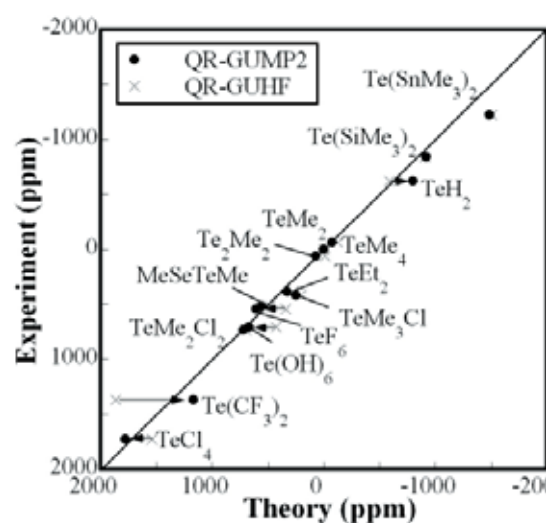


Fig. 1 Correlation between theoretical and experimental  $^{125}\text{Te}$  NMR chemical shifts.